Sonic Boom Excited Sediment Waves: A Model Study

H. K. Cheng,[1] J. A. Kunc,[1] and J. R. Edwards[2]

[1]Dept. Aerospace and Mechanical Engineering, Univ. Southern California, USA

[2]Acquisition Civil Engineering, Space & Missile System Center, Los Angeles AFB, USA

ABSTRACT

Sonic boom excited sediment waves are investigated with a model of interacting wave fields comprising water of finite depth and an elastic medium representing the sediment. The latter is assumed to be uniform, isotropic and semi-infinite in extent. The free modes are found to be dispersive, resulting in a finite (non-vanishing) resonance speed range. The study recognizes the difference in the far-field behavior between the excited resonance mode and the wave group of free modes: whereas the excited underwater wave of the resonance mode propagates at the same speed as the sonic-boom air load and remains in the form of a monochromatic wave train, the wave group of the free modes disperses into a wave packet and attenuate with increasing distance and time. Examples of a sediment model of fine sand with sonic boom waves at two flight Mach numbers are discussed. Differences and similarities between the present analysis and Desharnais and Chapman's study [1] are noted.

RÉSUMÉ

L'excitation d'ondes sédimentaires par le boom sonique est étudiée avec un modèle de champ d'ondes comprenant de l'eau de profondeur finie et un milieu élastique représentant le sédiment. Ce dernier est supposé uniforme, isotrope et d'étendu semi-infini. Les modes libres s'avèrent dispersifs, résultants une gamme finie de vitesse de résonance non atténuée. L'étude identifie la différence dans le comportement du champ lointain entre le mode de résonance excité et l'onde de groupe des modes libres: si l'onde sous-marine du mode de résonance se propage à la même vitesse que le boom sonique dans l'air et reste sous forme de train d'ondes monochromatiques, le groupe d'ondes des modes libres sont dispersés dans un paquet d'ondes et atténués avec l'augmentation de la distance et le temps. Des exemples d'un modèle de sédiment de sable fin avec des ondes de boomsonique à deux nombres de Mach de vol sont discutés. Des différences et les similitudes entre l'analyse actuelle et les travaux de Desharnais et de colporteur [1] sont aussi reportés.

1. INTRODUCTION

Many aspects of sound propagation in water can significantly affect the impact analyses of man-made noise underwater. [2,3]. This paper presents a model study of the transient, hydro-acoustic wave field in shallow water generated by a sonic boom over water and the resulting elastic-acoustic interaction that can excite sediment waves.

The problem of the underwater response to a sonic boom wave was modeled by Sawyers with a *flat* air-water interface [4] that has since been further elucidated [5], tested [6], and applied extensively.[7,8]. For convenience, Sawyers' model will be referred to as the "flat-ocean model". Tacitly assumed in Sawyers' analysis is an ocean of infinite depth not strictly applicable to the shallow coastal water. Aside from the effect of an impermeable bottom boundary, the interaction of a hydro-acoustic wave field with that of an elastic solid representing the sediment may excite seismic waves underwater [9-14] and could produce noticeable departures from Sawyers' prediction. Feasibility for sonic-boom-excited sediment waves was examined in the Desharnais and Chapman (D-C) paper [1] cited in the Abstract; the over-pressure signals received during the field test of a hydrophone array were identified to be disturbances originated from a Concorde airliner over-flight. Figure 1 reproduces from the D-C paper the over-pressure waveforms recorded at three depth levels and their comparison with the flat-ocean model prediction in this case. Except for the "ringing feature" on the downstream alluded to in Ref. [1], temporal averages of the over-pressure records tend to support Sawyers' prediction, as are made apparent from Fig. 1, even though the fluctuation/oscillation amplitudes are seen to be unexpectedly large. The analysis in the D-C study [1] employs a layered seismic model and indicates the existence of a resonance velocity not far from the reported Concorde

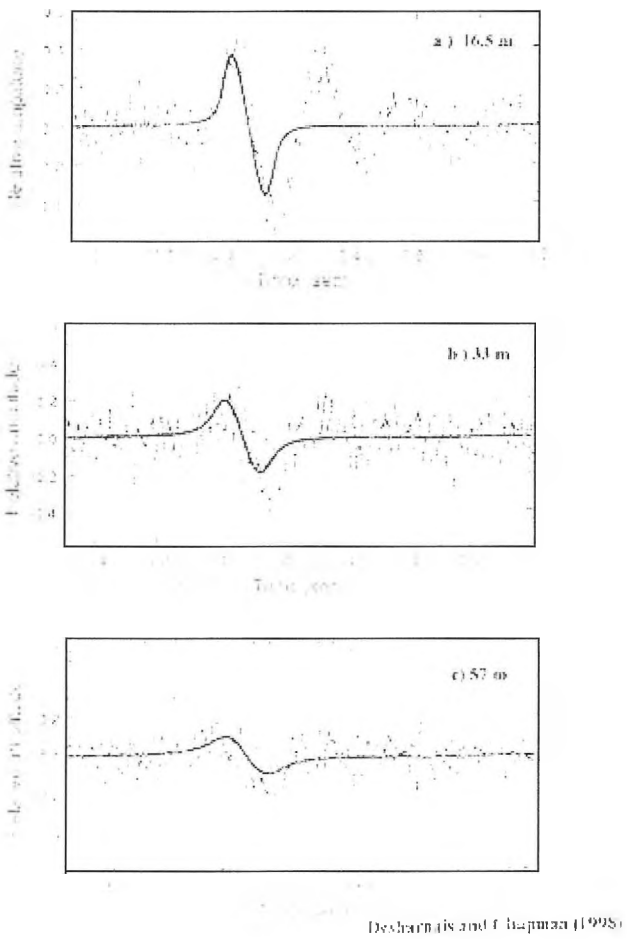

Figure 1. Overpressure waveforms recorded at three depth levels and their comparison with Sawyers' flat-ocean model predicted for a Concorde airliner overflight, reproduced from Desharnais and Chapman's paper [1].

flight speed. The study furnishes also certain spectral properties which appear to support the "ringing feature" mentioned earlier, although an alternative model based on an interaction mechanism involving a *wavy* air-water interface [15-18] could explain the ringing and other features of Fig.1. The present study holds, nevertheless, that the seismic interaction mechanism considered in the D-C paper addresses a new aspect of sonic boom underwater impact, and should add valuable understanding to the broader problem of sea-floor influence on underwater sound and noise. In the present work, a simpler model is used to analytically delineate the key interaction mechanism and to ascertain certain unique features found in the D-C study.

Additional remarks on the present work and the related studies are made below in Section 2 along with a description of the model and assumptions used in the analysis. The problem formulation is given in Section 3, followed by analyses of the wave-train problems in Section 4, where certain distinctions from classical studies [9, 10, 11] are noted, and the forced wave-train mode under a periodic transient air load is delineated. The latter is to be used as a generating function in the analysis in Section 5 for the more general, compact, transient air load. Here, the excited resonance mode as well as the transient response beyond the resonance range are studied; the distinctly different far-field behavior of the excited mode and the corresponding behavior of the free-mode group are compared. In Section 6, examples illustrating excitation of resonance sediment waves by an incident sonic-boom wave in and beyond the critical Mach-number range are discussed. Concluding remarks with further discussions are given in Section 7.

2. REMARKS ON THE MODEL

It is quite well known that the strong variation in shear rigidity of the sediment material is an important elastic property controlling sediment wave propagations [12, 14]. This was recognized in the D-C study [1], in which computations based on a layered model were made to simulate an elastic sea bed, assuming a power-law variation of the shear-wave speed with depth; the work accounted also for the presence of a shallow water above the sediment, which was included as one of the many layers in their computational study. As a paper complementing the D-C study, we examine the effect of a *finite* water depth for a simpler sediment model represented by a *homogeneous, semi-infinite* elastic medium. The latter, as mentioned, is amendable to detailed, analytical enquiries on its seismo-acoustic behavior under a transient, supersonic air load. The following presentation will show that the simpler model can reproduce salient features similar to those in the D-C study which may, perhaps, be better understood. The analysis shares the same physical model used in the classical analysis of underwater sound transmission over an elastic solid bottom [12, 13]. Unlike the latter which concern mainly a wave train in "free mode", the present analysis addresses wave fields excited by an incident sonic boom as a compact air load, and recognizes the distinct difference between the free-modes in group and the excited mode found with the transient air load.

A model with two spatial dimensions will suffice for the present study, by virtue of the extremely high aspect ratio generally found with sea-level sonic boom impact zones [15-18]. Figure 2 depicts the two interfaces separating the air, the water, and the sediment media, the Cartesian coordinates used, and together with some features of the mathematical model. Here, the plane $z = 0$ is made to coincide with the liquid-solid interface, while the plane $z = -h$ is identified with the air-water interface. Subscripts "1" and "2" used in the sketch and in the following will refer to the hydro-acoustic and the elastic media, respectively, while the subscript "A" refers to the air above water.

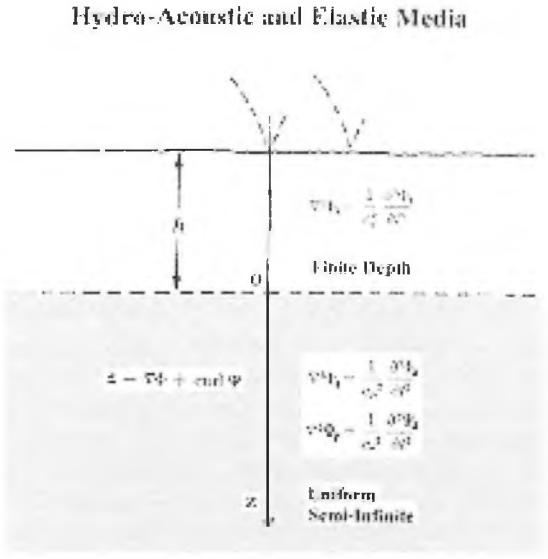

Figure 2. Schematic drawing depicting a planar hydro-acoustic medium of depth h and a semi-infinite elastic solid representing the sediment. In the coordinate system shown, the water-sediment interface and the air-water are identified at z = 0 and z = -h, respectively.

Implicitly assumed in Sawyers' theory as well as the present study are an extremely low air-to-water density ratio, $\rho_A / \rho_1 << 1$, and an air-to-water sound speed ratio less than unity, i.e. $c_A / c_1 < 1$. The first assumption makes the changes caused by the sonic boom in underwater fluid motion and in the air-water interface geometry negligibly small. The second assumption on sound speeds allows the underwater wave field to be treated as that in a *subsonic* flow, with the restriction that the Mach number M_A of the propagating sonic-boom wave field over water is less than c_1 / c_A. The latter has the value 4.53 under standard conditions. This restriction, $1 < M_A < 4.53$, will be observed here, as in References 1, 4-8, 15-18.

For the uniform isotropic media, Rayleigh and Stoneley/Scholte waves [9-11] correspond respectively to vanishing and infinite water depths, and are known to be non-dispersive [14a,b] in that their propagation (phase) speed do not depend on frequency/wave-number; this would limit the free-mode excitation to one *single* speed for a given set of sediment properties. Unlike these limiting cases, however, the free mode in the finite-depth problem at hand is *dispersive,* and there exists a non-vanishing (finite) speed range in which hydro-acoustic waves and sediment wave trains can be excited by a compact, transient air load. A finite and perhaps wider, critical speed range may, nevertheless, be expected for sediments modeled with layered or heterogeneous structure without the additional assumption of a finite water depth, as in Reference 1's model.

3. GOVERNING EQUATIONS

The task of analyzing the interaction problem of two spatial dimensions can be reduced to solving for three unknown functions: the displacement potential Φ_1 of the hydro-acoustic field, the scalar potential Φ_2 associated with the compressive-wave field and the horizontal component of a vector potential Ψ_2 associated with the shear-wave field of the elastic medium [12-14]. For the uniform isotropic media considered, each of these functions are governed by its own acoustics-like equation

$$\nabla^2\Phi_1 = \frac{1}{c_1^2}\frac{\partial^2}{\partial t^2}\Phi_1, \qquad \nabla^2\Phi_2 = \frac{1}{c_p^2}\frac{\partial^2}{\partial t^2}\Phi_2,$$

$$\nabla^2\Psi_2 = \frac{1}{c_s^2}\frac{\partial^2}{\partial t^2}\Psi_2 \qquad (3.1\ a,b,c)$$

where c_1 is the sound speed in water defined earlier; c_p and c_s are the compressional (wave) speed and the shear (wave) speed related, respectively, to the (Lame') compressional and shear moduli λ and μ, and the medium density ρ

$$c_p = \sqrt{\frac{\lambda + 2\mu}{\rho}} \quad \text{and} \quad c_s = \sqrt{\frac{\mu}{\rho}} \qquad (3.2a,b)$$

With the local displacement vector in the elastic medium represented by [13, 14]

$$\vec{d} = \nabla\Phi_2 + \nabla \times \vec{\Psi} \qquad (3.3)$$

the displacement continuity and the balance of the normal and tangential stresses across the (impermeable) horizontal, water-solid interface lead to three compatibility conditions at the interface z = 0:

$$\frac{\partial\Phi_1}{\partial z} = \frac{\partial\Phi_2}{\partial z} + \frac{\partial\Psi_2}{\partial x} \qquad (3.4)$$

$$-\rho_1\frac{\partial^2}{\partial t^2}\Phi_1 = \lambda_2\nabla^2\Phi_2 + 2\mu_2\left(\frac{\partial^2\Phi_2}{\partial z^2} - \frac{\partial^2\Psi_2}{\partial x\partial z}\right) \qquad (3.5)$$

$$0 = \frac{\mu_2}{\rho_2}\left[\left(\frac{\partial^2}{\partial x^2} - \frac{\partial^2}{\partial z^2}\right)\Psi_2 + 2\frac{\partial^2}{\partial x \partial z}\Phi_2\right] \qquad (3.6)$$

where the left-hand member of (3.5) is the over-pressure on the water side, and Φ_1 is the displacement potential. The latter is an integral of the velocity potential with respect to time t.

At the air-water interface z = -h (refer to Figure 2), the over-pressure in water must balance that of the air load which can be assumed to be given by the known, incident and reflected sonic boom waves. For the present study, it suffices to consider three types of air loads at z = -h

$$-\rho_1 \frac{\partial^2}{\partial t^2}\Phi_1 = 0 \qquad (3.7a)$$

$$-\rho_1 \frac{\partial^2}{\partial t^2}\Phi_1 = \rho_1 U^2 \alpha^2 \hat{P}_0\, e^{i(\alpha x - \omega t)} \qquad (3.7b)$$

$$-\rho_1 \frac{\partial^2}{\partial t^2}\Phi_1 = F(x - Ut) \qquad (3.7c)$$

pertaining to, respectively, the free mode, a transient sinusoidal air load, and a more general, non-sinusoidal, transient air load. The latter includes the over-pressure from a sonic boom. The propagation (phase) speed U of the air loads is assumed constant, and ω is αU. Results from the analysis for the air load of a sinusoidal wave train, (3.7b), will be used to generate solutions for the non-periodic, compact air load of interest. Since a semi-infinite elastic domain has been assumed, a vanishing Φ_2 and Ψ_2 at large z corresponding to the radiation condition will be required. With the use of the complex exponential functions in (3.7b) and in the following development, it is understood that these potentials and other quantities of physical interest are to be obtained from the *real parts* of the subsequent solutions.

The system of the three unknown functions Φ_1, Φ_2 and Ψ_2 are coupled through the interface compatibility conditions at z = 0, (3.4)-(3.6). The partial differential equations 3.1b and 3.1c for Φ_2 and Ψ_2 may also be coupled through additional terms in the equations, if the elastic moduli of the sediment were not uniform.

4. FREE AND FORCED WAVE TRAIN MODES

Solutions for the free mode and for the wave train mode forced by a sinusoidal air load of (3.7b) may be obtained in the wave train form

$$\begin{pmatrix}\Phi_1\\ \Phi_2\\ \Psi_2\end{pmatrix} = \begin{pmatrix}\hat{\phi}_1\\ \hat{\phi}_2\\ \hat{\psi}_2\end{pmatrix} \cdot e^{i\alpha(x-Ut)} \qquad (4.1)$$

The resulting ordinary differential equation (ODE) system for the three unknowns $\hat{\phi}_1$, $\hat{\phi}_2$ and $\hat{\psi}_2$, with the aforementioned compatibility and boundary conditions, is no more or less than that in the classical analysis for the submarine wave guide modeled with an elastic sediment [13], also in common with mathematical models used in studies of submarine earthquakes, mud slides and underwater explosions [13, 14]. The solutions sought and developed for the present study differ however from those of Reference 13 for reasons to be brought out shortly. The product of the wave number and the water depth, αh, will be an important parameter in the analysis but was absent from analyses of Rayleigh and Stoneley/Scholte waves [9-11].

The equations up to this point have been written in the *rest* frame. The following analysis will be made in a *moving* frame at the uniform horizontal velocity U. In this frame, the foregoing equations are unchanged, except that $\partial^2/\partial t^2$ is replaced by

$$\frac{\partial^2}{\partial t^2} + 2U\frac{\partial^2}{\partial x \partial t} + U\frac{\partial^2}{\partial x^2}$$

while the exponential argument i(αx-ωt) in (4.1) is changed to i(αx-Ωt) with Ω=Uα+ω. The velocity of the reference frame U is chosen to coincide with the phase velocity -ω/α so that the argument in (4.1) may become independent of time.

The underwater system admits solutions with "evanescent behavior"

$$\hat{\phi}_1 = A_1 e^{|\beta_1 \alpha| z} + A_2 e^{-|\beta_1 \alpha| z} \qquad (4.2a)$$

$$\hat{\phi}_p = B e^{-|\beta_p \alpha| z}, \hat{\phi}_s = C e^{-|\beta_s \alpha| z} \qquad (4.2b, c)$$

for *real* values of

$$\beta_1 = \sqrt{1 - M_1^2}\,,\ \beta_p = \sqrt{1 - M_p^2}\,,\ \beta_s = \sqrt{1 - M_s^2} \qquad (4.2d)$$

i.e. for $M_1 \equiv U/c_1 < 1$, $M_p \equiv U/c_p < 1$, $M_s \equiv U/c_s < 1$.

It could admit "effervescent" (propagating-wave) behavior like $e^{\pm i|\beta|\alpha z}$ if any of the βs becomes imaginary, i.e., if any of the three Ms exceed one. From the interface boundary conditions at $z = 0$ and $z = -h$, linear relations among the four constants A_1, A_2, B, and C, can be obtained. After eliminating A_2 and C, one arrives at

$$\left|\frac{\beta_p}{\beta_1}\right|\left(1-\frac{2}{2-M_s^2}\right)\cdot B + D_{BW}\cdot A_1 = 0 \qquad (4.3a)$$

$$\left[1+e^{-2|\beta_1\alpha|h}+D_{BW}\right]\cdot A_1 = \frac{\hat{P}_0}{\rho_1 U^2\alpha^2}e^{-|\beta_1\alpha|h} \qquad (4.3b)$$

where

$$D_{BW} \equiv -\frac{2}{1+\frac{\beta_1}{\beta_p}\frac{\rho_2}{\rho_1}M_s^{-4}\left[4\beta_s\beta_p-\left(2-M_s^2\right)^2\right]} \qquad (4.3c)$$

Note that D_{BW} is a function of U through M_s and the β s. The above result includes both the free and forced wave-train modes; the constant $\hat{P}_0$ in (4.3b) is set equal to zero identically for the free modes.

Note that the surface air load (prescribed over-pressure) on the air-water interface has been assumed, up to this stage, to be a sinusoidal one

$$p'(x,-h;\alpha) = \rho_1 U^2\alpha^2\cdot\hat{P}_0 e^{i\alpha x} \qquad (4.4)$$

Free Mode: Sediment Wave Train in Shallow Water

Unlike the Rayleigh and Stoneley/Scholte waves, for which the phase and group velocities are independent of the frequency or wave number, the free mode determined by

$$1+e^{-|\beta_1\alpha|h}+D_{BW}=0 \qquad (4.5a)$$

is *dispersive* in that its phase speed so determined will vary with the wave number, or more precisely, the product of the wave number and the water depth, αh. This leads to a non-vanishing (finite) range of the free-mode propagation speed, and thus a wider speed range for its excitation by a transient air load (see below) than in the Rayleigh and Scholte waves.

On the other hand, the dispersive property may produce a far-field behavior of a group of free modes very different from those of the non-dispersive Rayleigh and Stoneley waves (to be explained below). Equation (4.5a) may be more explicitly written in terms of the density ratio, the three Mach numbers and the product αh as

$$-\left(2-M_s^2\right)^2+4\sqrt{1-M_s^2}\sqrt{1-M_p^2} = \left(\frac{\rho_1}{\rho_2}\right)M_s^4\frac{\sqrt{1-M_p^2}}{\sqrt{1-M_1^2}}\tanh\left(|\beta_1\alpha|h\right) \qquad (4.5b)$$

which is identical in form with that for the fundamental (first) free mode of the water-channel wave guide with a solid floor of uniform elastic properties [13]. It reduces to the Rayleigh limit as $\alpha h \to 0$ and to the Scholte/Stoneley limit as $\alpha h \to \infty$. With a finite, non-vanishing h, the phase speed of the free mode (through M_1, M_p and M_s) now becomes a function of the wave number α. However, to be a genuinely free mode of the wave-train form (4.1), the wave number α and the propagation speed U must both be *real*; this sets a limit on the range of U admissible to (4.5b).

Values of $U(\alpha)$ satisfying the free-mode condition, (4.5b), for real α will be called the *free-mode speed;* it will be denoted by $U_{FM}(\alpha)$, wherever such a distinction is necessary. The wave field excited by a traveling air load at the critical speed will be referred to as the *resonance mode.* To be sure, $U_{FM}(\alpha)$ is the *phase* speed of the free mode observed in the *rest* frame. More significant, physically, is $\frac{d}{d\alpha}\left[\alpha\, U_{FM}(\alpha)\right]$ which approximates the *group velocity* in the far field and controls the evolution of wave packet formed by a group of free modes, to be delineated more fully in Section 5.

For a given density ratio ρ_1/ρ_2, the critical speeds for various different combinations of c_1, c_p and c_s may be found from (4.5b) for three kinds of combination of M_1, M_p and M_s. The first kind is one with all three Mach numbers being less than unity; however, the Mach number M_A above the air-water interface must remain $M_A < 4.53$. The second M-combination requires all the three Mach numbers to exceed unity, which would require a M_A very much greater than 4.53 in most applications, since the compressional speed c_p of the sediment is normally not much lower than the water sound speed c_1. The third combination requires $M_1 > 1$, $M_p < 1$ and $M_s < 1$ (supersonic in water, and subsonic in solid). The second and third kinds are not of great relevance to the sonic boom impact study and will not be considered in the subsequent analysis. (The third kind is similar to the Love waves in an elastic solid and could be of relevance to impact study of an intense explosion over a shallow sea.)

The admissible range of U_{FM}, or $(M_A)_{FM}$, for the free mode is determined by the upper and lower limits of the hyperbolic tangent in (4.5b) and may therefore be inferred from (4.5a) through

$$-2 < D_{BW} < -1 \tag{4.6}$$

From the free-surface condition (3.7a) and the solution (4.2a), the underwater over-pressure field in the moving frame is given by

$$p' = A_1[e^{|\beta_1\alpha|z} - e^{-2|\beta_1\alpha|h}e^{-|\beta_1\alpha|z}]e^{i\alpha x} \tag{4.7}$$

There can occur, more often than not, free-mode wave trains made up of α from a continuum wave-number range allowed by (4.5b). Such a wave group from the free-mode continuum is expected to undergo *attenuation* as it progresses (in time and space); this will be substantiated at the end of Sec. 5.

Wave Train Forced By Traveling, Periodic Air Load

With (4.3b) for a non-vanishing P_0, the constant A_1 of the potential in (4.2a) is determined; Applying the pressure-continuity requirement at the air-water interface (z = -h) once again, the constant A_2 of the potential may also be obtained, yielding

$$p' = \hat{q}e^{i\alpha x} \tag{4.8a}$$

and

$$\hat{q}(z,\alpha) = e^{-|\beta_1\alpha|(h+z)} + \frac{e^{-|\beta_1\alpha|(h-z)} - e^{-2|\beta_1\alpha|h}\cdot e^{-|\beta_1\alpha|(h+z)}}{\left(1 + e^{-2|\beta_1\alpha|h} + D_{BW}\right)} \tag{4.8b}$$

where the constant $\hat{P}_0$ has been taken to be unity, so that $\hat{q}$ = 1 at the air-water interface z = -h, satisfying the prescribed boundary condition there. The solution is regular as long as the propagation speed U of the air load is not close to the critical speed U_{cr} at which the denominator in (4.8b) vanishes.

5. RESPONSE TO MORE GENERAL, MOVING AIR LOADS

Solution as Fourier Integral

The product $\hat{q}e^{i\alpha x}$ is an underwater solution to the system with $p' = e^{i\alpha x}$ at z=-h, as is its weighted integral with respect to the wave number α

$$\frac{1}{\sqrt{2\pi}}\int_{-\infty}^{\infty} e^{i\alpha x}\hat{q}(z,\alpha)F(\alpha)d\alpha \tag{5.1}$$

where $F(\alpha)$ is an arbitrary weighting function. The correct choice for $F(\alpha)$ is one that will allow the weighted integral with respect to α to represent the over-pressure field in water under a traveling load $p'(x,-h)$. Since $\hat{q}(z,\alpha)$ approaches unity as $z \to -h$, this boundary condition simply requires that $F(-\alpha)$ be the Fourier transform of the interface air load $p'(x,-h)$.

$$F(-\alpha) = \frac{1}{\sqrt{2\pi}}\int_{-\infty}^{\infty} e^{i\alpha x}p(x,-h)dx \equiv P(\alpha) \tag{5.2}$$

Thus, under the assumption that the Fourier integral of the air load and the inverse Fourier transform of the product $\hat{q}P$ both exist, the solution in question is, for $-h < z < 0$,

$$p'(x,z) = \frac{1}{\sqrt{2\pi}}\int_{-\infty}^{\infty} e^{-i\alpha x}\hat{q}(z,\alpha)\,P(\alpha)\,d\alpha \tag{5.3}$$

where $\hat{q}(z,-\alpha) = \hat{q}(z,|\alpha|)$ has been given earlier by (4.8b) for the wave-train air load.

Rigid Bottom Result as Special Limit

Outside of the free-mode speed range allowed by (4.6) for the parameter D_{BW}, the function $\hat{q}(z,-\alpha)$ in (4.8b) has no singularity and the p' integral is expected to attenuate with increasing distance from the forcing air load, as in the case of a rigid bottom. The latter case corresponds to the limit of infinite compressive and shear speeds, in which D_{BW} vanishes. Equation (5.3) is reduced in this limiting case to

$$p'(x,z) = \frac{1}{\sqrt{2\pi}}\int_{-\infty}^{\infty} e^{-i\alpha x}\frac{\cosh\beta_1|\alpha|z}{\cosh\beta_1|\alpha|h}P(\alpha)\,d\alpha \tag{5.4}$$

which represents an extension of Sawyers' [7] analysis to shallow water and provides an alternative solution form to the rigid sea-floor problem given earlier in References 17, and 18.

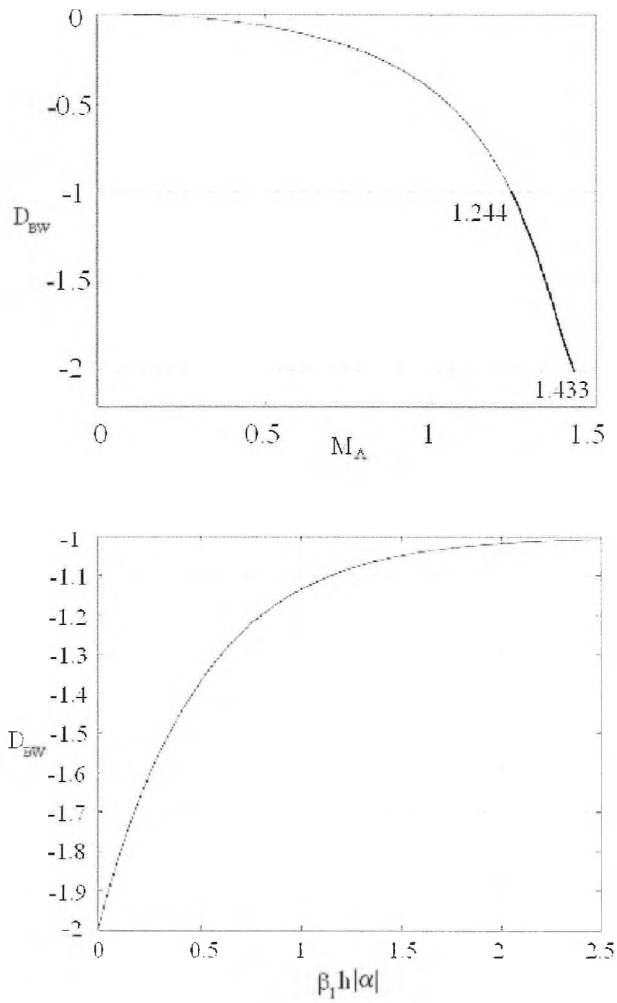

Figure 3. Illustration of diagrams used for determining of the air Mach number $M_A \equiv U / a_A$ corresponding to the free-mode phase velocity $U_{FM}(\alpha)$ for a wave number α through the function $D_{BW}(U)$, which can also be used to determine the specific wave number α_* in an excited resonance mode for a known air-load velocity U: (a) D_{BW} as function of M_A, (b) D_{BW} as function of $\beta_1 h|\alpha|$. The example shown was computed from $\rho_1/\rho_2 = 1.91$, $c_p = 1711\,\mathrm{m/s}$, and $c_s = 503\,\mathrm{m/s}$.

The Excited Resonance Modes

For a traveling air-load at speed U which falls inside the range allowed by (4.6), the integration path of (5.3) encounters the pole singularity of $q(z,\alpha)$ at the particular wave number α^* corresponding to U in the free-mode requirement (4.5b). This particular wave number α^* is therefore a function of the air-load velocity U, and will appear in solution pairs to the nonlinear algebraic equation (4.5b) for a given U. Examination of the relation between the exponential function in arguments β, α, h and the $D_{BW}(U)$ of (4.5a) indicates that only a single pair of real $\alpha^* = \alpha_{FM}(U)$ in the form of $\alpha^* = \pm|\alpha^*|$ is possible for a given U (cf. Fig. 3). This fact provides the basis for the following analysis. The analysis will also make use of the fact the the function $p'(x,-h)$ prescribed for the transient air load at the air-water interface is a *real* function of x.

Essential to the contributions from the poles is the behavior of the denominator of $q(z,\alpha)$ (cf. (4.8b))

$$\Delta \equiv 1 + D_{BW} + \exp(-2h\beta_1|\alpha^*|) \tag{5.5}$$

whose behavior near α^* differs according to whether α^* is positive or negative. The function $\hat{q}(z,a)$ in the vicinity of the two poles $\alpha = \pm a$ may thus be represented by

$$\hat{q} \approx \frac{g_*(z,a)}{2\beta_1 h}\frac{1}{1+D_{BW}}\frac{1}{\alpha \mp a} \tag{5.6a}$$

where $g(z,a)$ is the limit for $|\alpha| \to a$

$$g_*(z,a) = \lim_{|\alpha|\to a} g = 2e^{-2\beta_1 ha}\sinh(\beta_1 a(h+z)) \tag{5.6b}$$

Recognizing that $P(-a)$ is the complex conjugate of $P(a)$, the excited overpressure field in water ($-h < z < 0$) may be re-expressed with the help of (5.6a,b) around the two poles, as[¥]

$$p'(x,z) = -\sqrt{\frac{\pi}{2}}\frac{g_*(z,a)}{\beta_1 h}\frac{sign(x)}{1+D_{FM}} * \mathbf{RP}[iP(a)e^{-iax}] + \frac{1}{\sqrt{2\pi}}\int_{-\infty}^{\infty} e^{-i\alpha x} Q(z,\alpha;a)\,d\alpha \tag{5.7a}$$

where "**RP**" stands for the Real Part and

$$Q(z,\alpha;a) = \hat{q}(z,|\alpha|)P(\alpha) + \frac{g_*(z,a)}{2\beta_1 h}\frac{1}{1+D_{BW}}\left(\frac{P(a)}{\alpha - a} - \frac{\overline{P(a)}}{\alpha + a}\right) \tag{5.7b}$$

[¥] In deriving (5.7a), use was made of the identity

$$\frac{1}{\sqrt{2\pi}}\int_{-\infty}^{\infty}\frac{e^{-i\alpha x}}{\alpha}d\alpha = -i\sqrt{\frac{\pi}{2}}\,sign\,x\,.$$

The existence of the inverse Fourier transform of Q requires regularity of $P(\alpha)$ along the real axis of α. The two poles in question are thus removed from the remaining integral. Note that the overpressure p' in (5.7a) is to be obtained from the *real part* of the equation's RHS. For large water depth p' of (5.7) may be seen to diminish as *1/h*. On the other hand, for small water depth, p' of (5.7) does not diminish with *h*, owing to the fact that both $\Delta\hat{q}$ and g_* vanish linearly with h (for $-h < z < 0$).

The above result represents the resonance mode in water excited by a traveling air load. Examples most befitting to this description are those found in sonic boom over flat (non-wavy) water, for which the air load is readily determined. A standard example of this kind will be examined in section 6.

Excited Far Field

At large distance (x>>1) from the air load, the integral in (5.7), which is the inverse Fourier transform of *Q*, *vanishes* for a wide class of *Q* which is *absolutely integrable* with respect to α.[20] The latter condition can be met by a $P(\alpha)$ which is *regular* along the real axis of α. Thus as $|x| \to \infty$, p' of (5.7) assumes the form of a free mode at a *specific* wave number pair $\alpha = \pm a$ corresponding to the air-load speed *U*. Rewriting (5.7) for coordinates in the rest frame, the overpressure in water *far* from the air load becomes

$$p'(x,z,U) \sim -\sqrt{\frac{\pi}{2}}\frac{g^*(z,a)}{\beta_1 h} * \\ sign(x-Ut)\mathbf{RP}\{\frac{iP(\alpha)e^{i\alpha(x-Ut)}}{1+D_{FM}}\} \qquad (5.8)$$

where *a* and D_{FM} are functions of *U*, and $g_*(z,a)$ is a function of both *U* and *z* (for the same set of sediment properties). The *monochromatic* character of this far-field resonance mode has a special significance for its *non-attenuating* nature. This behavior must be considered *distinct* from the shallow water free modes which are allowed to occur arbitrarily over a wide range of α. The combined effect of the free-mode wave *group* is expected to result in attenuation with distance and time, and warrants a closer examination to be made presently.

Free-Mode Group: Comparison

Physical realization of the free modes of (4.5)-(4.7) depends on the initial data or a prior production process (such as a finite-energy release) which normally involves a broad wave-number band. With the (rare) exception of a (very) narrow-band α-distribution, the wave group of the free modes, instead of (4.7) for a single mode, takes the form

$$p' = \frac{1}{\sqrt{2\pi}}\int_{-\infty}^{\infty} A(\alpha)\cdot e^{i\alpha[x-U_{FM}(\alpha)t]}e^{-\beta_1 h|\alpha|}\cdot \\ \sinh[\beta_1 h(1+z/h)|\alpha|]d\alpha \qquad (5.9)$$

for an arbitrary integrable $A(\alpha)$. The far field behavior of this integral along each ray of constant *x/t* is determined by the stationary phase, tantamount to the group velocity

$$\frac{d}{d\alpha}[\alpha U_{FM}(\alpha)] = x/t \equiv \eta \qquad (5.10)$$

and thereby attenuates as the inverse square root of $|x|$ or t [19-21]. More specifically, the non-coherent free-mode group (5.9) disperses and transforms itself into a packet of wavelets, each of which propagates along a "ray" of constant *x/t* with a fixed wave number/frequency at the group velocity, and attenuates according to the "cylindrical spreading rule" [19-21].

$$p'(x,z',t) \sim \frac{E_*}{\sqrt{2|\Omega_*''t|}} exp\, i\alpha_* * \\ \left\{[x-U_{FM}(\alpha_*)t]+\frac{\pi}{4}(sgn\,\Omega_*'')\right\} \qquad (5.11a)$$

where the asterisk denotes the stationary value $\alpha = \alpha_*$ satisfying (5.10),

$$\Omega \equiv \alpha U_{FM}(\alpha),\ \Omega'' \equiv d^2\Omega/d\alpha^2 \qquad (5.11b,c)$$

and

$$E \equiv A(\alpha)e^{-\beta_1 h|\alpha|} * \\ \sinh[\beta_1 h(1+\frac{z}{h})|\alpha|] \qquad (5.11d)$$

Owing to their dispersive property, the free modes of (4.5)-(4.7) occurring in group differ significantly in the far-field behavior from the free mode of the Rayleigh wave or the Stoneley wave. To the latter, the far field of the excited resonance mode (5.8) is also similar, but differs in having a broad-band resonant U-range (4.6) that neither the Rayleigh nor the Stoneley wave enjoy.

6. EXAMPLES: SONIC BOOM EXCITED SEDIMENT WAVES

Sonic Boom N-wave as Air Load

A standard form of $p'(x,-h)$ in sonic boom prediction method is that of an N-shape. In terms of the normalized x-variable based on the sonic boom signature length (say, L'), it can be written as

$$p'(x,-h) = (1-2x)I(x)I(1-x) \qquad (6.1a)$$

where $I(\xi)$ denotes the unit-step function of ξ, and the overpressure p' is normalized by its maximum/peak value. The normalized x and p', together with the dimensionless z as well as the Fourier variable α are all be made dimensionless with L' in the example study below.

The Fourier transform of $p'(x,-h)$ in this case is

$$P(\alpha) = \frac{1}{\sqrt{2\pi}\,(i\alpha)} * \left[(e^{i\alpha} - 1)(1 + \frac{2}{i\alpha}) - 2e^{i\alpha}\right] \qquad (6.1b)$$

which is *finite* and *regular* (containing no pole) at the origin $\alpha = 0$, and vanishes as $1/\alpha$ for large α. These behaviors assure the existence of the integral solution (5.3).

Sediment Properties Selection

The range of U permitted by (4.5b) for resonance, and its existence, depends on the density ratio ρ_1/ρ_2 and the characteristic speeds c_1, c_p and c_s. More critical is the sediment shear speed c_s which is the lowest among the three characteristic speeds and controls the 4th power of M_s on the RHS of (4.5b). Resonance may be expected to occur when U and c_s are comparable. Three sediment samples are selected from measured and computed properties of mud and sand to show the variety in ρ_1/ρ_2, c_p and c_s (Cf. Table 8.2.1 Reference 22 and shown below). The sound speeds in air and water in the model study are taken to be c_A =331 m/sec and c_1 =1500 m/s, respectively. The range of U or the air Mach number M_A permitted by (4.5a,b) corresponding to (4.6) for resonance, can be determined from the listed density ratio and the characteristic speeds for sediment models I, II and III as

$$1.24 < M_A < 1.44,$$
$$0.52 < M_A < 0.56,$$
$$4.52 < M_A < 4.53 \qquad (6.2\ a, b, c)$$

respectively. The following discussion will focus on examples illustrating underwater responses of sediment Model I to sonic booms at speeds within and outside the above M_A range. Model II would support sediment wave trains for moving air load at subsonic speed as well. Interestingly, resonance may still be found even with shear speed as high as in the sediment model III, although the resonance-speed range is extremely narrow, as indicated by (6.2c). Examples with sediment models II and III will not be included for discussion below.

Supersonic Over-flights at M_A = 1.5 and M_A = 1.36

The case of M_A =1.5 outside the resonant range (6.2a) is first examined. To render the results more relevant, the reference length scale L' for x, z and h can be taken to be 100m, which is not far from the sonic boom signature of the Concorde airliner. With the set of constants assumed for data set I, we have ρ_2/ρ_1 =1.91, M_1=0.331, M_p=0.290, M_s=0.987, β_1=0.944, β_p=0.957, β_s=0.160, and D_{BW}=-15.41. In addition, the water-layer depth is taken to be *twice* the signature length, i.e. h = 2, a depth of 200 m.

The waveform at the sea level for an incident N-wave is shown in Figure 4a where the normalized maximum overpressure was set equal to 0.33. The underwater waveform at mid channel (i.e. z = -1) with the rescaled $p'(x)$ for the N-wave is shown in Figure 4b. Not shown for this case is the over-pressure on the sediment boundary (z =0), of which the magnitude is uniformly less than 10^{-3} of the surface value at x = -h. As expected, no evidence of interaction involving the sediment medium can be found in this case. In fact, the result differs little from that of a rigid, flat-bottom wall and appears to be very similar to results obtained for rigid bottom walls given in References 7, 8, and 16.

Next, we examine the results for M_A=1.36 which falls within the M_A-range of (6.2a) for which ρ_2/ρ_1=1.91, M_1=0.300, M_p=0.263, M_s=0.895, β_1=0.954, β_p=0.965, β_s=0.445, D_{BW}=1.09, and h=2. The latter corresponds to a water depth of 200 m. The normalized overpressure waveforms at the water surface z= -h = -2, at mid channel z = -h/2 = -1, and on the bottom z = 0. are presented in Figures 5a, 5b, and 5c, respectively. Unlike the results shown earlier for M_A=1.5, undiminished sinusoidal oscillations at large distances in the form anticipated by

Table 1. Sediment Characteristics. (From Reference 22)

		ρ_2/ρ_1	c_p (m/s)	c_s (m/s)
I	Very fine sand (continental terrace)	1.91	1711	503
II	Clay (Abyssal hill)	1.42	1491	195
III	Uralite Basalt (Kolan rock)	3.06	6580	3660

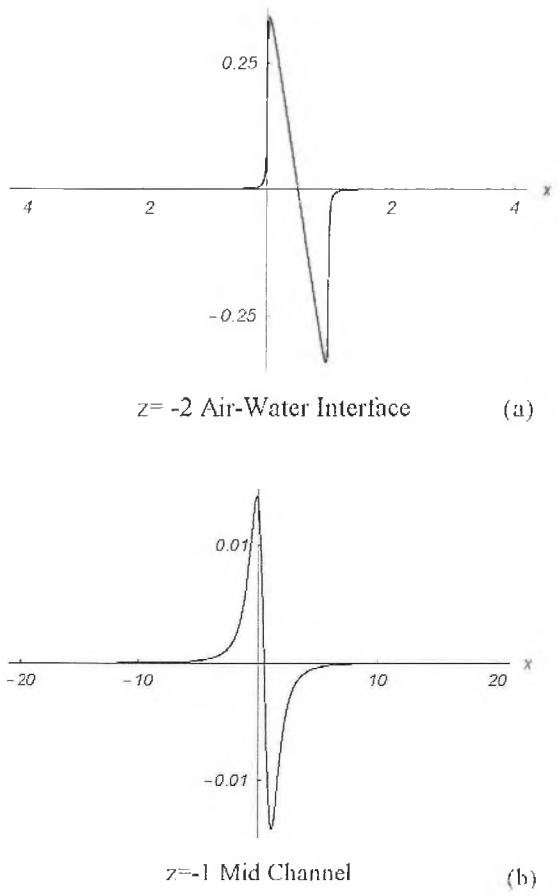

Figure 4. An example of hydro-acoustic response of the water-solid system to an incident sonic boom at $M_A = 1.50$ which is outside the resonance-speed range $1.24 < M_A < 1.44$ for a normalized water depth h=2, $\rho_1/\rho_2 = 1.91$, $c_p = 1711\ \mathrm{m/s}$, and $c_s = 503\ \mathrm{m/s}$; overpressure are shown at (a) sea level (z=-h=-2), (b) mid channel (z=-h/2=-1). Result at sediment boundary (z=0) not shown (Cf. text).

(5.8) appear at both the lower depth levels. The periodic oscillation in overpressure on the sea floor ($z = 0$) is seen to have *twice* the amplitude as that at mid-channel ($z = -h/2 = -1$), indicating clearly that the monochromatic, non-attenuating disturbances has been generated from the interaction at the lower boundary and radiate upward as if from a new acoustic source at the bottom. One may apply the results, for example, to the case with a maximum overpressure p' at the sea level equal exactly to 0.33 pounds per square foot (psf), the oscillatory p' amplitude at the mid channel and channel bottom would accordingly be close to 0.017 psf and 0.031 psf, respectively. These magnitudes correspond to sound levels close to, and slightly higher than,

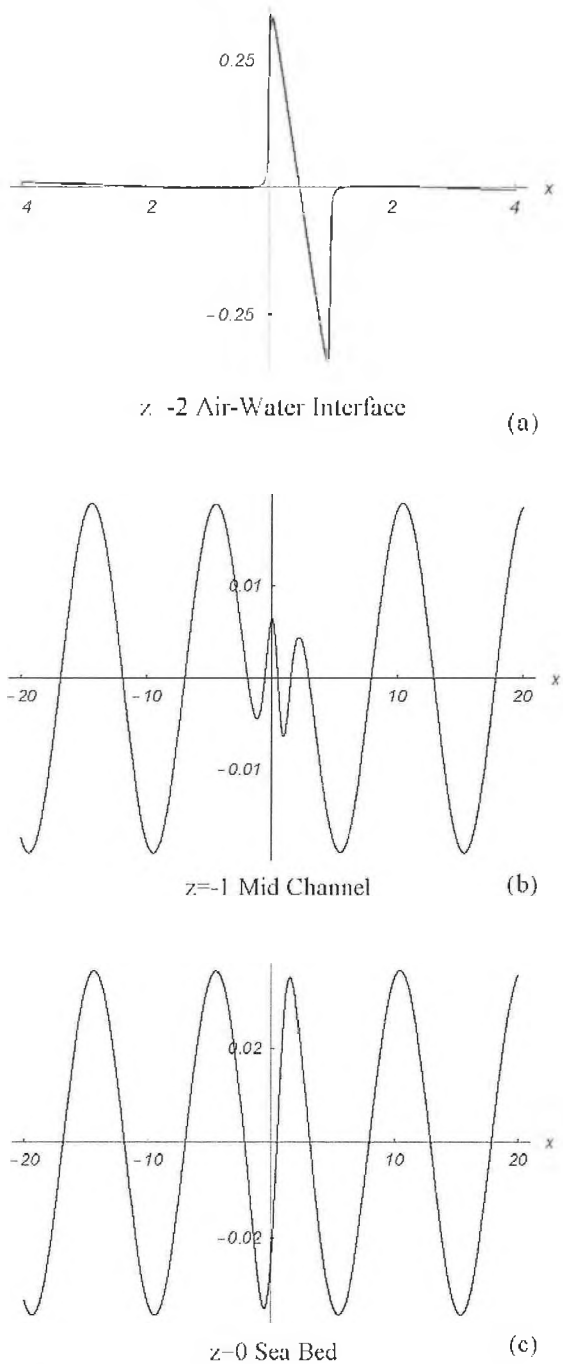

Figure 5. An example of sonic-boom excited sediment waves in a water-solid system same as in the proceeding figure, except $M_A = 1.36$ which falls within the resonance speed range ($1.24 < M_A < 1.44$): (a) sea level (z = -h = -2), (b) mid channel(z = -h/2 = -1), and (c) sediment boundary (z = 0).

120 dB (re 1 μPa), which may be compared with the levels of recorded whale calls in the infrasound range [2, 3].

Further Discussion

Two features of interest may be noted in Figures 5a, 5b, and 5c. The noticeably long wave length shown in Figures 5b, and 5c, which is $\lambda \equiv 2\pi / \alpha$, normalized by the sonic boom signature length, indicates that the excited wave length is nearly ten times the signature length. This should not be a surprise, however, after examining how $\alpha^*(U)$, or more precisely, how $2\beta_1 h\alpha^*$, is determined from a given U in the range $-2 < D_{BW} < -1$ (cf. Figure 3). A typical U well within the admissible range is seen to give an α^* pair corresponding to a $2\beta_1 h\alpha^*$ in the unit-order range, i.e. to a wavelength

$$\lambda^* \approx 4\pi\beta_1 h \qquad (6.3)$$

This is numerically large, indeed, and suggests that the λ^* nearly ten (10) in length shown in Figures 5b, and 5c must have resulted from a $2\beta_1 h\,|\alpha^*|$ value comparable to 1/3. Therefore the apparently high numerical value comparable to that of (6.2) is not unexpected in the shallow water *far field* ($|x|>>1$). It is unclear if similarly long wavelengths were found in the corresponding results in the D-C study [1], since data were not furnished for far ($x>>1$) locations.

In the near field [$x=O(1)$] on the other hand, a characteristic wave length of unit order is expected.. This expectation finds support in the mid-channel result ($z=1$) of Figure 4b, where a relatively weak oscillation with a unit-order wavelength comparable to that of the sonic boom signature occurs in $x=O(1)$, while the solution is expected to approach the prescribed N-profile as z tends to the air-water interface $z=-h$. In the D-C study, it was reported that their spectral solution in the higher wave-number end appears to amplify with distance from the sediment boundary ($z=0$). The mid-channel result at $x=O(1)$ and related observation noted above could provide an explanation of the seemingly peculiar feature of the result in Reference 1 noted above, even through substantial differences exist between their model and the present one.

Unresolved among the reasons/cause for the differences between measurement records and model predictions are the absence of "ringing" on the upstream side and the presence of a large pressure over-shoot on the downstream side, which was revealed evidently in Figure1a (reproduced from Figure 5a of Reference 1).

7. CONCLUDING REMARKS

Sonic boom excited resonant interaction of the hydro-acoustic wave field and the elastic wave field of the ocean sediment is studied with a model of flat, uniform shallow sea over a homogeneous (uniform), semi-infinite, elastic solid. The finite depth h of the shallow water renders its free propagation mode dispersive when observed in a moving frame, allowing a family of free modes and a non-vanishing range of resonance speed for a traveling air load. For a rigid ocean bottom, the need for correcting Sawyers' theory [4] for applications to shallow coastal water is obvious, and this needed modification appears explicitly as a special limit in the present analysis [cf. (5.4)].

With suitable combination of sediment density, compress ional and shear speeds, the critical speed range of supersonic over-flight for the resonance interaction can be found. The hydro-acoustic field structure and the resonance condition (when the flight speed falls within the free-mode speed range) have been analytically studied for the far and near fields. Computed results for over-flight speeds within and outside the resonance–speed range were examined. Distinctions of the resonance mode analyzed from the Rayleigh and Stoneley waves and from the corresponding D-C study, have been noted. Significant differences between the shallow-water *free* modes and the *excited* resonance mode with regard to their far-field behavior have been recognized. The examples studied suggest not only that, with low enough shear-wave speed on the sediment, the excitation event in question is realizable, but also that the undersea sound level can be comparable to, or even higher than, that of the recorded infrasound from whale calls [2,3].

Similar behavior of the excited resonance mode can be expected of the D-C analysis; the layered sediment model assumed therein would introduce additional dispersive effects, as in most sediment wave studies involving heterogeneous media [14]. It is of interest to note that the values of $c_p = 1600\ \mathrm{m/s}$ and $\rho_2/\rho_1 = 1.8$ assumed in the D-C study were rather close to the corresponding values 1711 *m/s* and 1.91 of the sediment model (set I) used for the examples of Fig 4a,b. An important difference lies, of course, in the layer-approximation simulating the non-uniform shear-speed distribution assumed in Reference 1, namely, $c_s = 160(\bar{z})^{0.3}$, where $\bar{z}$ is in meters. If a typical shear speed value is to be taken from this power law at the representative location, say, $\bar{z} = 50\mathrm{m}$, one would obtain $c_s = 517\ m/\sec$, not far from the 503 *m/sec* in the present example. The Concorde airliner in question was estimated to cruise at Mach 1.75, corresponding to M_A at the air-water interface of M_A=1.5. The latter is not too far from the upper limit 1.44 for excitation for the present model (6.1a). As the discussion in Section 6 would suggest, several outstanding discrepancies between measurements and model predictions may not be resolved completely within the frame work of the flat-water model.

In conclusion, we consider the model of sonic-boom excited sediment waves proposed originally by Desharnais

and Chapman [1] to have physical merit; the phenomenon is worthy of more critical studies for a wider class of sonic boom impact problems. Among the latters are the extension of a shallow-water analysis to account for the shear-speed non-uniformity, as well as a study of the evolution process of the steady-state free modes. New field measurements and laboratory studies will be necessary to resolve issues of the earlier and new measurements and to help in developing a viable prediction model. A fuller presentation of this work is given in a report entitled "A Model Study of Sonic Boom Excited Sediment Waves," available on the author's website [23].

ACKNOWLEDGEMENT

The senior author would like to acknowledge the valuable exchange and advice on the subject from D. Chapman, C. S. Clay, F. Desharnais, D. Erwin, O. Godin, C. Greene, C. J. Lee, Y. G. Li, H. Medwin, R. Nigbor, and L. Redekopp. Helpful assistance was provided by T. Y. Hsu and B.Wang. The work is based on research performed under the Ocean Sonic Boom Program sponsored by the Institute for Environment, Safety and Occupational Health Risk Analysis, Brook AF Base, and the Environmental Management Div. Acquisition Civil Engineering of the AF Space Missile and Space System Center, Los Angeles, through Parsons Engineering Science Subcontract 738249.3000-000, to HKC Research during July 2000-August 2001.

REFERENCES

[1] Desharnais, F. and Chapman, D.M.F. (2002) "Underwater Measurement and Modeling of a Sonic boom", *J. Acoustic Soc. Am.,* vol.111 (1), Pt.2, 2002, pp.540-553

[2] Richardson, W. J., Greene, C.R., Jr., Malme, C.I. and Thompson, D.H. (1995) *Marine Mammals & Noise*, Acad. Press, pp.15-86,525-552.

[3] ARPA, NOAA and State of Hawaii (1995) Final Environ. Impact Statement for the Kauai Acoustic Thermometry of Ocean Climate Project and its Assoc. Marine Mammal Res. Program, *ARPA, NOAA & Univ. Calif., San Diego* vols. I & II.

[4] Sawyers, K.H. (1968) "Underwater Sound Pressure from Sonic Boom", *J. Acoustic Soc. AM.*, vol.44, no.2, pp.523-524.

[5] Cook, R. (1970) "Penetration of a Sonic Boom into Water", *J. Acoustic Soc. Am.*, vol.47, no.3, pt.2, pp.1430-1460.

[6] Interier, P. F. and Malcolm, G. N. (1973) "Ballistic Range Investigation of Sonic Boom Overpressure in Water", *AIAA J.*, vol. 11, no. 4, pp.510-516. .

[7] Sparrow, V.W. (1995) "The Effect of Aircraft Speed on the Penetration of Sonic Boom Noise in Flat Ocean", *J. Acoustic Soc. Am.*, vol.97., pp.159-162.

[8] Sparrow, V.W. and Ferguson, T. (1997) "Penetration of Sharp Sonic Boom Noise into a Flat Ocean", *AIAA,* paper 97-0486.

[9] Rayleigh, J.W.S. (1887) "On Waves Propagating Along the Plane Surface of an Elastic Solid", *Proc. London Math. Soc.*, vol.17, pp.4-11.

[10] Stoneley, R. (1924) Proc. Royal Soc. (London), Ser. A, vol.160, pp.416.

[11] Scholte, J.G.J. (1947) "The Range of Existence of Rayleigh and Stoneley Waves", Monthly Notices of the Royal Astronomical Soc., Geophysical Supp., vol.5, pp.120-126. (Reprint Dover Pub. 1944)

[12] Stoll, R. D. (1986) *Sediment Acoustics*, Lecture Notes in Earth Sciences, Springer-Verlag.

[13] Tolstoy, I. and Clay, C.S. (1966) *Ocean Acoustic*, McGraw Hill.

[14] Aki, K. and Richards, P.G. (2002) *Quantitative Seismology* 2nd Ed. Univ. Science Books, Sansalito, CA.

[15] Cheng, H.K. and Lee, C.J. (2000) "Sonic Boom Noise Penetration Under a Wavy Ocean: Part I. Theory" Univ. Southern Calif. Dept. Aerospace and Mechanical Engineering, *USC AME Report* 11-11-2000; documented on website "http://www-rcf.usc.edu/~hkcheng"

[16] Cheng, H.K., Lee, C.J. and Edwards, J. (2001) "Sonic Boom Noise Penetration Under a Wavy Ocean: Part II. Examples and Extensions". Univ. Southern Calif. Dept. Aerospace & Mechanical Engineering *USC AME Report* 4-4-2001.

[17] Cheng, H.K. (2001) Final Report of Experimental and Theoretical Investigations on Ocean Sonic Boom Propagations, HKC Research, Los Angeles, CA.

[18] Cheng, H.K. and Lee, C.J. (2002) "Sonic Boom Noise Penetration Under a Wavy Ocean: Theory", (under review for publication in *J. Fluid Mechanics*); available at website "http://www-bcf..usc.edu/~hkcheng".

[19] Lighthill, M.J. (1978), *Waves in Fluid*, Camb. Univ. Press, pp.249-250.

[20] Lighthill, M.J. (1958, 1964), *Fourier Analysis and Generalized Functions,* Cambridge Univ. Press.

[21] Lighthill, M.J. (1965), "Group Velocity", *J. Inst. Math. & Applications*, vol.I, pp.1-28.

[22] Clay, C. S. and Medwin, H. (1977) *Acoustical Oceanography,* John Wiley & Son, p. 258.

[23] Cheng, H. K., Kunc, J. A. and Edwards, J. R. (2003), "A Model Study of Sonic Boom Excited Sediment Waves", Univ. Southern Calif. Dept. Aerospace & Mechanical Engineering *USC AME Report* 6-6-2003. http://www-rcf.usc.edu/~hkcheng

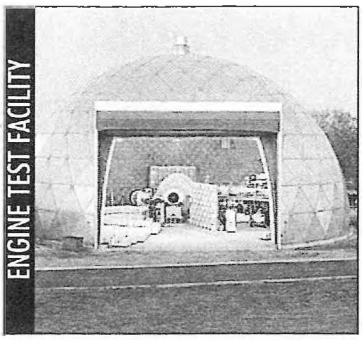

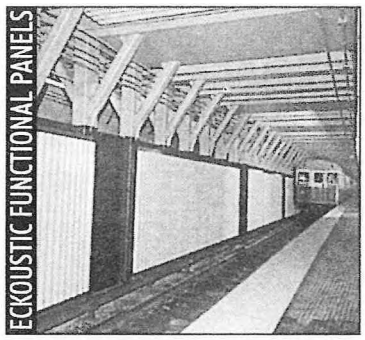

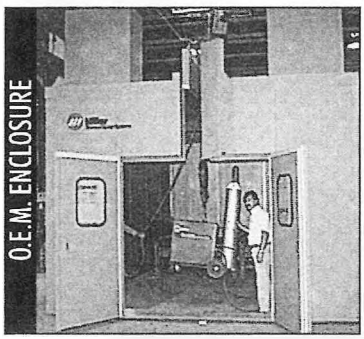

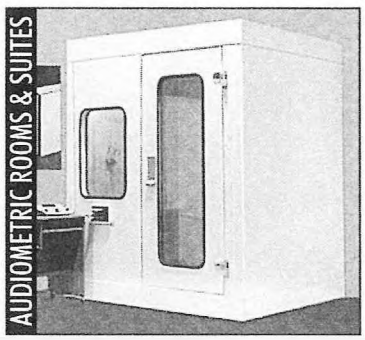

SOUND SOLUTIONS FOR THE FUTURE

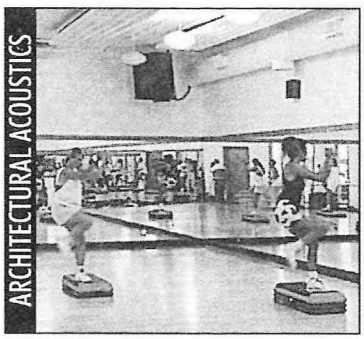

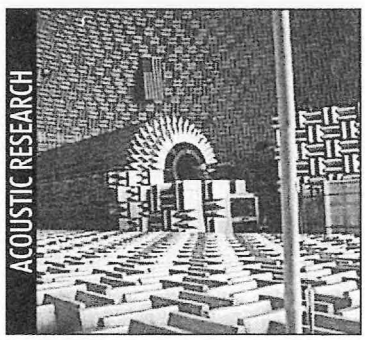

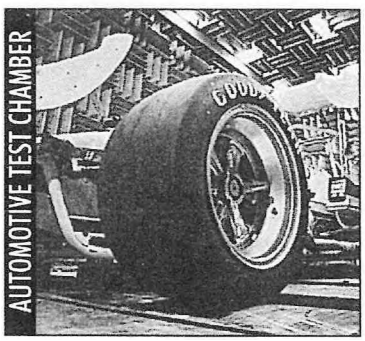

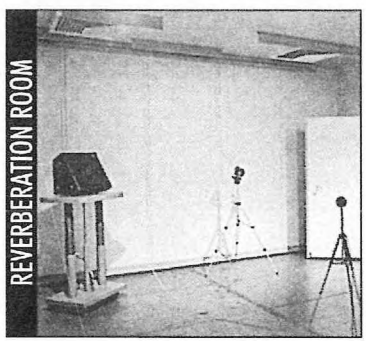

ECKEL

NOISE CONTROL TECHNOLOGIES

CANADIAN OFFICE
Box 776 100 Allison Avenue Morrisburg ON K0C 1X0
Tel: 613-543-2967 800-563-3574 Fax: 613-543-4173
Web site: www.eckel.ca/eckel e-mail: eckel@eckel.ca

NOISE CONTROL TECHNOLOGIES

Gunnar Rasmussen Acoustic Solutions:

Precision Acoustic Measurement Instrumentation

New Products

ICP Powered Microphone Prea
Ear Simulation Devices
Speech Simulation Devices

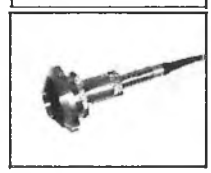

Condenser Microphones and Preamplifiers
Intensity Probes
Outdoor Microphones / Hydrophones
Calibration Instrumentation and Accessories

G.R.A.S.
Sound & Vibration

Represented in Canada by

NOVEL DYNAMICS INC.
Dynamic Test and Analysis Systems

Integrated Solutions from World Leaders

Novel Dynamics Inc.
Phone 519-853-4495 Fax 519-853-3366
Email: metelka@aztec-net.com
Ottawa Office 613-599-6275 Fax 613-599-627